

Phase behaviour and non-periodic crystallisation of random aromatic copolyesters and their side chain bearing systems

Z. He^{*}, F.J. Davis, R.H. Olley, G.R. Mitchell

J.J. Thomson Physical Laboratory, University of Reading, Whiteknights, Reading RG6 2AD, UK

Received 20 June 2000; received in revised form 1 December 2000; accepted 5 December 2000

Abstract

Two series of semiflexible aromatic copolyesters have been prepared and studied. In the first series, the relative proportion of a biphenyl and a phenyl unit was varied through copolymerisation; in the second, the phenyl ring system was further substituted with an aliphatic side-chain, in order to promote additional disruption to any solid-state ordering. These copolymers have been characterised experimentally. The phase behaviour and morphology were closely inspected using a variety of techniques including wide angle X-ray diffraction, optical and scanning electron microscope and differential scanning calorimetry. The copolymers are proposed to be randomly copolymerised through a comparison of the results from X-ray diffraction with those from modelling. The modification of polymer repeat units alters the properties of the final polymers dramatically. Crystallisation of the copolymers is complicated. The rate of crystallisation is reduced through the introduction of side chains. The crystallisation behaviour is explained using a non-periodic lattice model by lateral matching of the similar units. Despite the low degree of polymerisation of the copolymers examined, the results do, nevertheless, point to a route whereby the properties of the polymeric systems in general may be controlled through molecular engineering. © 2001 Elsevier Science Ltd. All rights reserved.

Keywords: Aromatic copolyesters; Crystallisation; Side chain

1. Introduction

The continuing search for polymers with improved or unusual properties has led to a considerable level of interest in the behaviour of so called rigid-rod polymers; i.e. polymers built up from aromatic units connected by suitable functionality. Such materials are of interest because of their potential to form fibres of particularly high strength [1–3]. Probably the most well-known class of rigid-rod polymers are the aromatic polyamides; Kevlar [4], for example, has achieved commercial success in a variety of applications, especially those which rely on its unique combination of high strength and low density [5].

The major drawback to the commercial exploitation of many rigid-rod systems is their lack of processibility. The factors which give rise to high mechanical strength, in particular the high level of rigidity imparted to the system by the aromatic sub-structure, unfortunately also restricts the number of conformational arrangements available to the poly-

mer chain; both in solution and in the molten state. Thus, rigid-rod polymers tend to exhibit low solubility and high melting points [6]. The problem is often compounded by the fact that the materials are often semi-crystalline, as a consequence of the intrinsic linearity of the polymer backbone and the high levels of interaction between neighbouring chains.

Several approaches have been used in an attempt to improve the processibility of rigid-rod polymer systems. Unfortunately, these often result in materials of lower rigidity, or with a less rod-like structure. For example, modification of Kevlar, by changing the *para-para* linkages to *meta-meta* results in a more soluble material, but one with a substantially reduced moduli [7]. Substantial changes to the linear material can be introduced by adding small quantities of the meta substituted monomer into a predominantly *para* chain [8].

The nature of the linkages between the aromatic groups in a polymer also has a marked influence on the phase behaviour. If complete conjugation is maintained then the materials become extremely intractable, and may exhibit electrical conductivity, as in poly(*p*-phenylene) [9,10]. In aramid systems, conjugation is limited, but the rigidity is enhanced by intermolecular hydrogen bonding between the amide linkages. In contrast, for polyesters, the corresponding interactions are dipolar in nature, and therefore reduced;

^{*} Corresponding author. Present address: School of Engineering, Napier University, 10 Colinton Road, Edinburgh EH10 5DT, UK. Tel.: +44-131-4552211; fax: +44-131-4552264.

E-mail address: z.he@napier.ac.uk (Z. He).

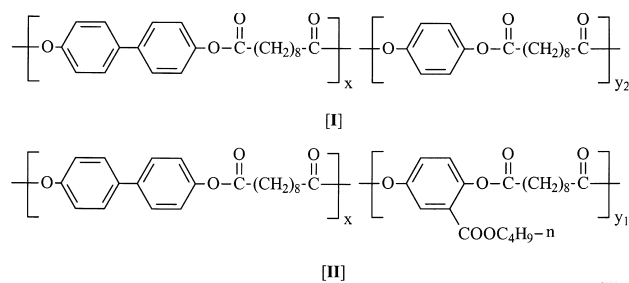
the materials are, as a consequence, often more processible. A further increase in the degree of flexibility may be achieved by adding long (often methylene) chains between the aromatic units. The additional freedom thereby introduced into the molecule results in materials with markedly reduced phase transition temperatures, often showing liquid crystalline behaviour [11].

The degree of crystallization of a rigid aromatic polymer can be substantially reduced by introducing an additional (often rather similar) unit into the polymer backbone in a copolymerisation reaction [12]. It is well-known that copolymerisation reduces the crystalline melting points of polymers. As early as 1947 Flory [13,14] proposed a statistical model of such behaviour. In Flory's model the comonomers may be considered as randomly distributed points at which crystallization cannot occur, thereby reducing the number of the longer crystallites. Often for rigid rod systems the reduction of crystallinity is not as marked as might be expected on the basis of Flory's simple theory. More recently it has been shown that crystallization may be observed, even in random copolymers containing high concentrations of two different aromatic units. In such systems, heterogeneous crystallites may be formed based on the matching of identical sequences of the two units in a non-periodic lattice [15,16].

One further approach to improving the processibility of rigid rod polymers is to introduce side-groups to the aromatic polymer [17]. Such side-groups may typically consist of alkyl chains and the additional degree of conformational entropy introduced, serves to increase the solubility and decrease the melting point of the polymers. A further influence of the side-groups may be to reduce crystallization via the steric restriction of close contact between neighbouring chains. Unfortunately, a reduction of crystallinity will be accompanied by a reduction in the mechanical strength of the solid polymer, and particular care must be taken to ensure a balance between the favourable effect of side-groups on processibility and the unfavourable effects on properties. In this contribution, we further [18,19] examine the role of side-groups attached to rigid aromatic polymers through a comparison of a series of polymers and copolymers, both with- and without side-chain bearing units. We shall use these as a model to allow further understanding of the complex relationship between phase behaviour and structure in aromatic polymer systems.

2. Materials

The polymers synthesized here were polyesters formed by the reaction between an acid chloride and varying proportions of a mixture of 4,4'-biphenol and either hydroquinone or butyl 2,5-dihydroxybenzoate. The resultant polyesters formed the two series of copolymers shown in Scheme 1. These contained either a mixture of biphenyl and phenyl rings linked by a long chain alkyl group, labelled PB_nQ_m , or biphenyl rings and a single aromatic ring containing a butyl ester side-chain,



Scheme 1.

labelled PB_nCB_m . For simplicity the homopolymers are labelled as PB10, Q10 and CB10 with the letter denoting the appropriate ring. It was the intention of these investigations to determine the consequences of varying proportions of a side-chain unit on a relatively rigid polymer chain. We have attempted to separate this effect from the statistical effect of copolymerisation by a comparison of the two series. The PBQ series will show effects arising from the disorder occurring as a consequence of the introduction (in a random copolymerisation — see later) of the two ringed biphenyl system and the single ringed quinol unit. In the PBCB series the additional influence of the side chains can be monitored.

3. Experimental

3.1. Material preparation

The polymers synthesized here were polyesters formed by the reaction between Sebacoyl chloride and an equimolar mixture of 4,4'-biphenol and either hydroquinone or butyl 2,5-dihydroxybenzoate in varying proportions. Biphenol was obtained from Aldrich and used without further purification. Sebacoyl chloride was distilled under reduced pressure (124–125°C, 0.7 mmHg) prior to use. Butyl 2,5-dihydroxybenzoate was prepared from 2,5-dihydroxybenzoic acid via acid catalysed esterification as follows:

2,5-dihydroxybenzoic acid (18.8 g, 0.12 mole), butanol (23 ml, 0.25 mole), and concentrated sulphuric acid were refluxed in toluene (dried over sodium, 25 ml) in a flask fitted with a Dean–Stark attachment for 8–9 h. When the reaction was complete (no more water was produced), the product was poured into water and extracted with diethyl ether. The ether extract was washed with saturated sodium hydrogen carbonate solution, dried and the solvent evaporated. The resultant solid was recrystallized twice from petroleum ether, accompanied by treatment with decolorising charcoal, to yield 10 g (39%) of butyl 2,5-dihydroxybenzoate. $^1\text{H NMR}$ (60 MHz, CDCl_3): = 1.0 (3H, t), 1.6 (4H, m), 4.3 (2H, t), 5.5 (1H, s), 6.9–7.3 (3H, m), 10.3 (1H, s). I.R (cm^{-1}): 3350 (b), 1668 (s).

Copolymers: Polyesters were obtained [20] from the interfacial polymerization of sebacoyl chloride and varying proportions of the required phenolic compounds. Particular care was taken to ensure that the total concentration of

Table 1
Solubility of the PBCB and the PBQ polymers

Polymers	Solvent (g per 100 g solvent) ^a				
	CHCl ₃ (50°C)	CH ₂ Cl ₂ (warm) ^b	THF ^c (50°C)	DMF ^d (50°C)	DMAc ^e (50°C)
PB10CB0	i	i	i	i	
PB9CB1	p			i	
PB5CB5	> 0.06	p	p	p	p
PB2CB8	> 1.8	> 3.9	> 1.3	> 3.9	> 1.3
PB0CB10	s (*)	s (*)	s (*)	s (*)	> 1.3
PB9Q1	i			i	
PB5Q5	p	i	p	i	p
PB2Q8	> 0.04	p	p	p	p
PB0Q10	> 0.04	p	p	P	~0.3

^a **i**, insoluble, **p**, partially soluble, **s**(*), soluble but not quantified.

^b The low boiling point prevents measurement at 50°C.

^c Tetrahydrofuran.

^d Dimethyl formamide.

^e Dimethyl acetamide.

aromatic phenol was identical to that of the diacid chloride; any differences would result in lower molecular weights for the final polymers. A typical example of the procedure used, in this case for the 'homopolymer' between sebacoyl chloride and biphenol, is given below.

Biphenol (2.0 g, 0.011 mol) was dissolved in oxygen-free sodium hydroxide solution (0.34 N, 62 ml). The solution was then placed in a commercial blender and tetrabutylammonium hydrogen sulphate was added to act as a phase transfer catalyst. To this aqueous phase was then added an organic phase, consisting of sebacoyl chloride (2.3 ml, 0.011 mole) dissolved in ethanol-free chloroform. The two-phase mixture was then stirred at high speed for about 5 min (adding additional water as required), transferred to a beaker and heated to remove the chloroform. The crude polymer was collected and transferred to a Soxhlet extractor and extracted with methanol to remove unreacted monomer and low molecular weight material.

3.2. Measurements

DSC measurements were performed on a Perkin Elmer DSC-2C equipped with a MC² [4] data processing system. Optical microscopy was performed using a Jena-Zeiss microscope equipped with a variable temperature stage. The X-ray diffraction apparatus has been described elsewhere [21]. The molecular calculation was performed on a silicon graphics workstation using CHARMM/Quanta programs. The theoretical calculation on the diffraction pattern was based on the RU-PRISM program. For morphological studies, specimens were etched with a solution of potassium permanganate in orthophosphoric acid according to a published method for PEEK [22], and examined using a Philips SEM 515 electron microscope with an accelerating voltage of 10–12 keV.

4. Results and discussions

4.1. Polymer characterisation

Solubility: Solubility is of course one of the major measures of the processibility of a polymer. In this work, the polymers were tested in a variety of solvents and the results are shown in Table 1. From the results, it is clear that only the polymers containing high concentrations of side-chain bearing units exhibit significant (or useful) solubility. Although they are semi-quantitative in nature, it is interesting to note that the 50:50 side-chain containing system was not as soluble as the one containing a higher proportion of side chains. This clearly reflects the increased effectiveness of the side chain units at enhancing solubility compared with the randomisation associated with copolymerisation (see later).

Composition: Due to the low solubility in common solvents, the composition of the polymers was measured by careful analysis of the infra-red spectra of the materials. In this approach a peak was selected, which was diagnostic of the presence of the biphenyl ring at 1007 cm⁻¹; this was compared with a peak present in all examples, choosing that at 1755 cm⁻¹, arising from the carbonyl absorption.¹ The ratio of the two peaks could be related to the concentration of biphenyl units in the polymer. The results obtained are listed in Table 2; it can be seen that, where comparisons are possible, the results obtained from infra-red measurements are in good agreement with those obtained from NMR data. For the PBCB series the results are broadly in line with expectations on the basis of the concentrations in the initial polymer feedstock; for the PBQ series the concentration of biphenyl is rather lower than might be expected.

¹ The absorption from the carbonyls in the main chain was distinct from those due to the side-chain carbonyls at 1728 cm⁻¹ and from any remaining carboxylic acid at 1709 cm⁻¹.

Table 2

Yield of polymerisation and experimentally determined compositions and molecular weights of the PBCB and PBQ polymers (Note: An estimation of errors for the composition measurements is about $\pm 10\%$. An estimation of errors for the degree of polymerisation and molecular weight are about $\pm 10\text{--}40\%$)

Polymers	Yield (%)	Compositions (%)									Molecular weight					
		Feedstock compositions			NMR measurements			FTIR measurements			FTIR measurements		GPC measurements			
		<i>x</i>	<i>y</i> ₁	<i>y</i> ₂	<i>x</i>	<i>y</i> ₁	<i>y</i> ₂	<i>x</i>	<i>y</i> ₁	<i>y</i> ₂	$\langle DP \rangle_n$	$\langle M \rangle_n$	$\langle M \rangle_n$	$\langle M \rangle_w$		
PB10	90	100	0	–	–	–	–	–	–	100	0	–	10.6	3700	–	–
PB9CB1	90	90	10	–	–	–	–	–	–	77	23	–	7.0	2500	–	–
PB5CB5	79	50	50	–	44	56	–	–	–	52	48	–	4.6	1700	–	–
PB2CB8	68	20	80	–	21	79	–	–	–	23	77	–	3.5	1300	1930	3650
CB10	56	0	100	–	–	–	–	–	–	0	100	–	4.6	1700	1990	4650
PB9Q1	87	90	–	10	–	–	–	–	–	90	–	10	10.1	3500	–	–
PB5Q5	77	50	–	50	–	–	–	–	–	36	–	64	7.2	2200	–	–
PB2Q8	67	20	–	80	–	–	–	–	–	15	–	85	7.3	2100	–	–
Q10	51	0	–	100	–	–	–	–	–	0	–	100	8.0	2200	–	–

Molecular weight: As a consequence of the poor solubility of the materials, only the two polymers containing the highest concentrations of side-chain bearing units were sufficiently soluble to obtain data from GPC measurements. For the remainder of the samples, an estimate of the number average degree of polymerisation and hence molecular weight were obtained from the solid samples by infra-red spectroscopy. Here the estimate was based on the relative intensities of the band assigned to the main-chain ester linkages at 1755 cm^{-1} , and that attributed to the acid end groups at 1709 cm^{-1} . For the side-chain containing series, particular care had to be taken to correct for the contribution of the side-chain ester linkages to the overall absorption in the appropriate region of the infra red spectra. The molecular weight data obtained for the materials synthesised here is also shown in Table 2, as can be seen the values were found to be particularly low in all cases. It should be noted, however, there is a large degree of uncertainty in the data; although where comparison between GPC and IR data is possible there is reasonable agreement.

4.2. Room temperature X-ray diffraction

The solid state structure of these copolymers was examined using wide-angle X-ray diffraction. Fig. 1 shows scattering intensity as a function of S , the scattering vector,² for the range of copolymers (as prepared) studied.

For the PBCB series (i.e. the side-chain containing copolymers) the X-ray diffraction curves (Fig. 1a) show 2-major peaks. In all samples, the most intense peak was at $S = 1.51\text{ \AA}^{-1}$ (2θ , 21.2°). The position of this peak is independent of the composition, but the peak became broadened and the amorphous scattering contribution raised as CB (i.e. the shorter unit with side chain) composition of the copolymer increased. A series features was observed at low S

($\sim 0.4\text{ \AA}^{-1}$). The peak position varied from $S = 0.32\text{ \AA}^{-1}$ (2θ , 4.5°) of PB10 to $S = 0.45\text{ \AA}^{-1}$ (2θ , 6.3°) of CB10 and it was most intense for high fraction of PB, i.e. PB10.

For PBQ series (i.e. copolymers without side chains), the X-ray diffraction peak at $S \sim 1.51\text{ \AA}^{-1}$ was similar to the PBCB series (Fig. 1b). The position was insensitive to the compositions, but peak broadening (or two peak overlapping) was observed when the phenyl concentration was high, in particular in the Q10 sample. As with its PBCB series, a peak at low S ($\sim 0.4\text{ \AA}^{-1}$) was observed. Its position varied from $S = 0.32\text{ \AA}^{-1}$ of PB10 to $S = 0.44\text{ \AA}^{-1}$ (2θ , 6.1°) of Q10 and the peak was most intense for both homopolymers, i.e. PB10 and Q10.

The peaks detected in these samples may be assigned to their specific structural features as follows:

4.2.1. Diffraction at $S \sim 1.5\text{ \AA}^{-1}$

The X-ray diffraction peak at $S \sim 1.51\text{ \AA}^{-1}$ can be related to the correlation between neighbouring polymer chains, i.e. the lateral packing of repeat units. The invariant feature of the diffraction peak indicates both copolymer series have very similar lateral packing distance and it is unaffected by both types of structural modification. This lateral packing distance between main chain was calculated, which is $\sim 4.2\text{ \AA}$.

In the side chain containing system, however, although the peak position is invariant with compositions, there is a systematic broadening as the fraction of CB unit increases. This broadening indicates a reduction of long range order in the polymer system, which can be quantified using a correlation length, ΔL .³ Table 3 shows a steady reduction in ΔL as the proportion of the side chains increases; the side chains enforce a disruption to the crystallisation in the PBCB polymer system. In the non side-chain containing system, PBQ series, the correlation length is approximately constant for those materials with a greater proportion of the biphenyl

² $S = 4\pi \sin \theta/\lambda$, where 2θ is the angle between the incident and scattered beams, and λ is the wavelength of the incident radiation (i.e. 1.542 \AA).

³ $\Delta L = 2\pi/\Delta S$, where ΔS is the breadth of the peak at half its maximum intensity of the peak.

Table 3

The measured peak width and the correlation length calculated from X-ray diffraction at $S = 1.51 \text{ \AA}^{-1}$

Polymers	$\Delta S (\text{\AA}^{-1})$	$\Delta L (\text{\AA})$
<i>As prepared</i>		
PB10CB0	0.15	42
PB9CB1	0.16	39
PB5CB5	0.18	35
PB2CB8	0.23	27
PB0CB10	0.25	25
<i>As prepared</i>		
PB9Q1	0.15	42
PB5Q5	0.16	39
PB2Q8	0.23	27
<i>Annealed</i>		
PB10CB0	0.13	48

ring (Table 3). At higher concentrations of the shorter component broadening is observed. However, unlike PBCB series, this broadening should be seen as the presence of overlapping peaks due to obvious peak splitting in the Q10 polymer. Such twin peaks are a common feature of X-ray scattering patterns in main-chain aromatic polymers [23,24] and have also been seen in benzene [25]. The two peaks are thought to arise from different packing distances due to a face-to-face contact between neighbour planar aromatic units. The equivalent correlation cannot be seen in biphenyl systems because of the twisted nature of the two rings. So is in the side-chain containing system, presumably for steric reasons, the face-to-face contact is not allowed.

4.2.2. Diffraction at $S \sim 0.4 \text{ \AA}^{-1}$

The peak at $S \sim 0.4 \text{ \AA}^{-1}$ can be related to the correlations along the chain. Hence the introduction of the shorter ring system decreases the length of the repeat unit and therefore, the diffraction peak shifts to a slightly higher value of S .

In a copolymer system, how an ordered structure could exist along a copolymer chain direction and give a certain diffraction peak, is not a straightforward question. Mitchell and Windle [26,27] introduced a simple method to explain the presence of the sharp intrachain peaks in the scattering patterns of copolymers. In the copolymer studied here, the system is considered as a one-dimensional chain containing two chemical units of different lengths, r_a and r_b , and of differing compositions.

The lengths of the different repeat units were estimated from molecular models generated using molecular mechanics (CHARMm) level energy minimisation. They were found to be $r_a = 20.6 \text{ \AA}$ (for PB10) and $r_b = 16.8 \text{ \AA}$ (for Q10). Simple interpretation of the experimentally observed peak positions for the two homopolymers PB10 and Q10 gave values for r_a and r_b are 19.6 and 14.5 \AA . The difference may arise from a tilted packing arrangement or from a non-extended flexible spacer conformation.

The results of calculation of the scattered intensities based on the model of Mitchell and Windle [26,27] using

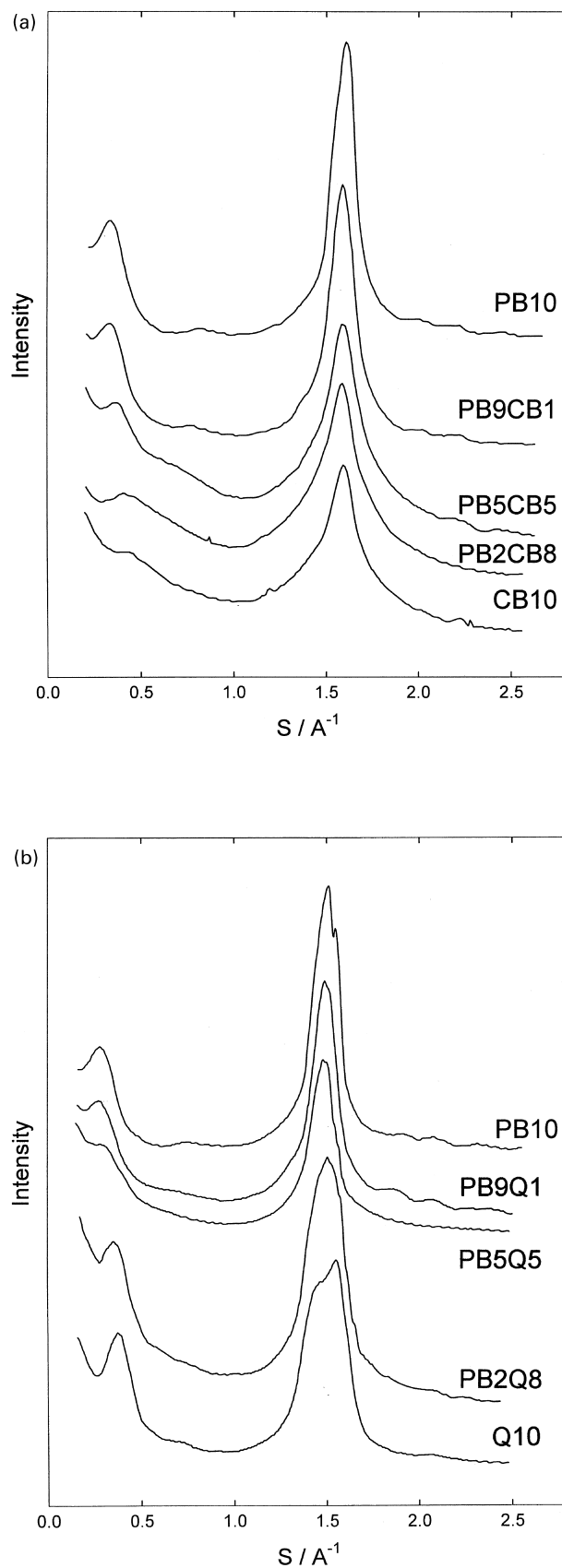


Fig. 1. X-ray diffraction patterns obtained at room temperature from: (a) PB-CB and (b) PB-Q copolymers.

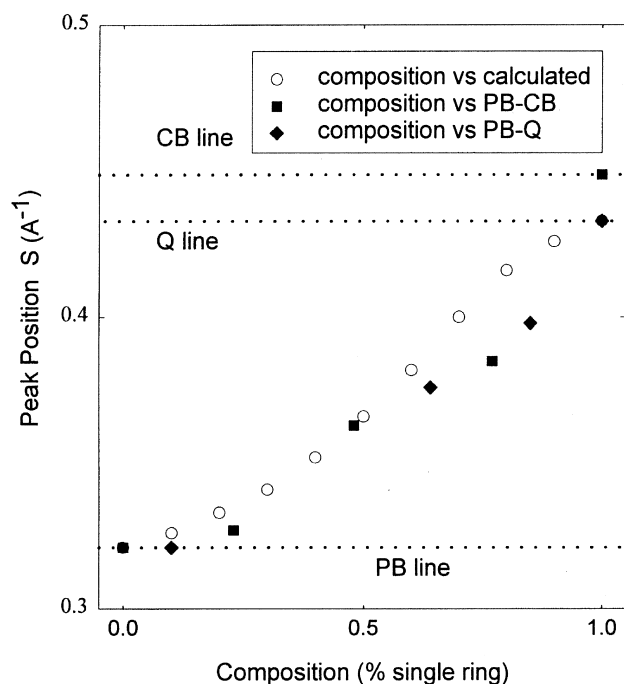


Fig. 2. A comparison of the theoretical analysis of X-ray diffraction for a random copolymer and the experimental results of low angle range X-ray diffraction of the PBQ and PBCB copolymers.

point scattering function are shown in Fig. 2. The model takes as input the values of $r_a = 19.6$ and $r_b = 14.5$ Å and the fraction of each repeat unit (Table 2). Clearly the data series does not fit the prediction for a block copolymer system. However, the fit to a random copolymer model is not complete for systems with a high proportion of the single ring repeat unit. This could reflect in part some variation in reactivities of the monomers or difference in the tilt angle of the mesogen in the chain.

Given the greater difference between the calculated molecular length for Q10 and that obtained from the experiment, the latter explanation appears to have more weight. It is clear that the complete lack of fit between the block copolymer model and the data eliminates that possibility. The modest but broad agreement between the fully random copolymer and the data suggests that we should consider these two series (PB-CB and PB-Q) as largely random copolymers.

4.3. Thermal transitions

In order to understand the thermal transitions and their structure relation from these materials, both differential scanning calorimetry and optical microscopy were used,

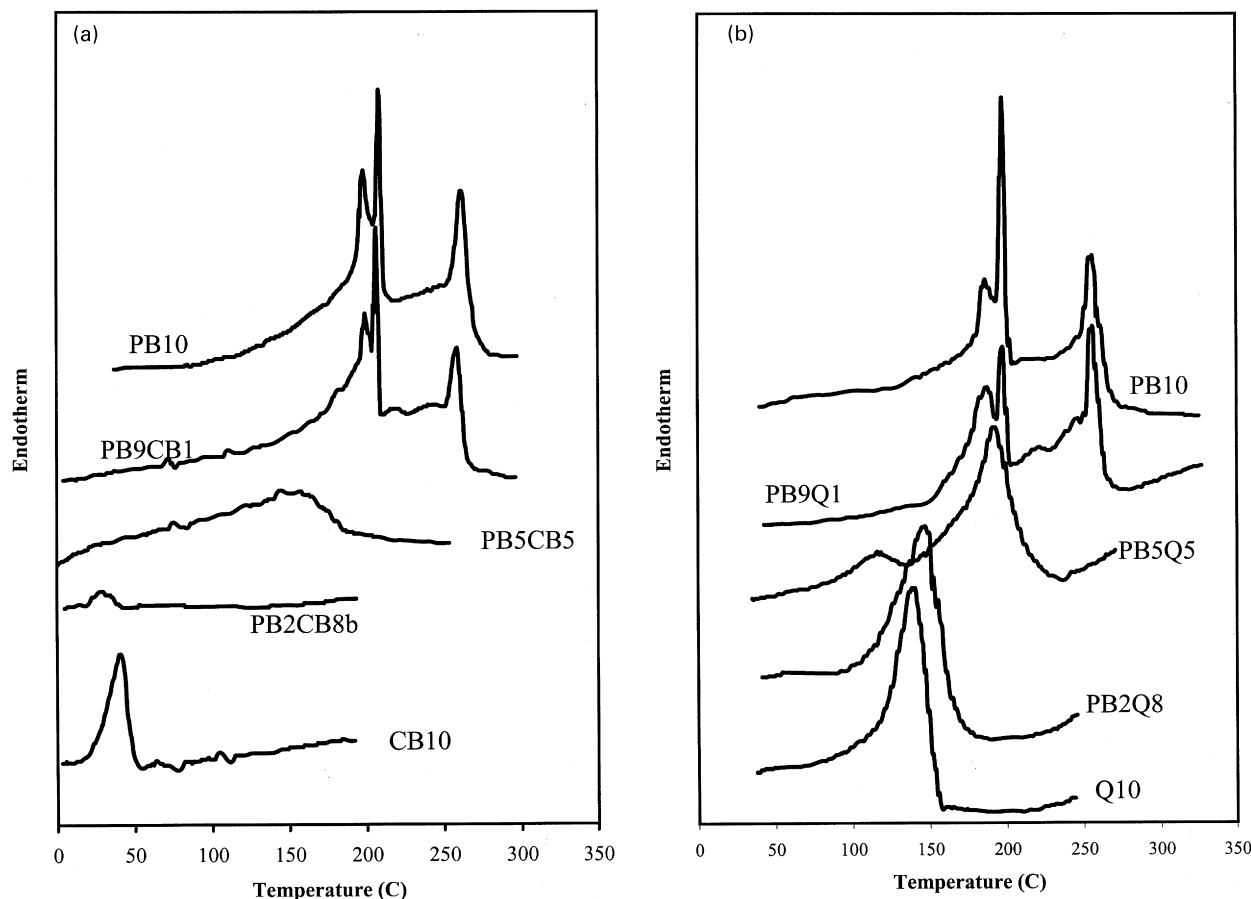


Fig. 3. DSC curves obtained at a scanning rate of $20^\circ\text{C min}^{-1}$ during the second heating from the scan-cooled samples of (a) the PB-CB copolymers and (b) PB-Q copolymers.

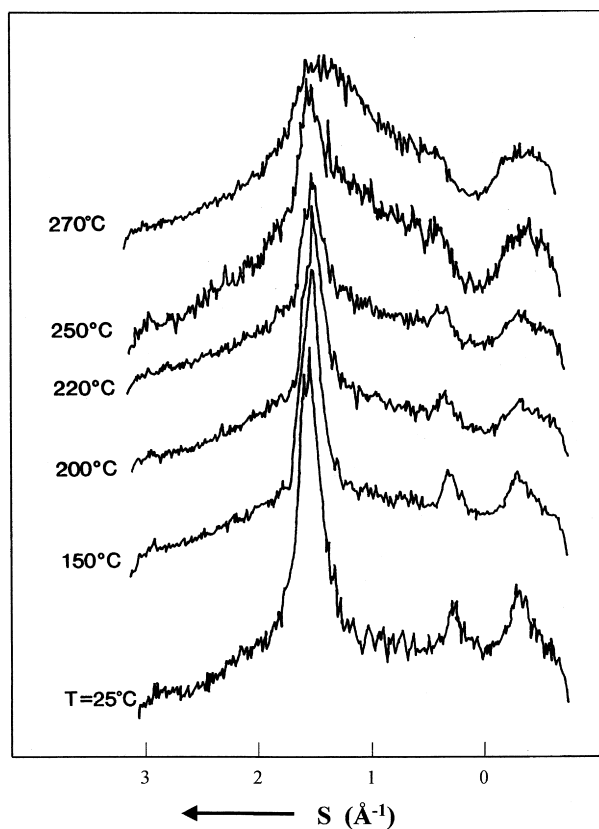


Fig. 4. X-ray diffraction patterns changes with temperature for the PB10 polymer.

in addition to X-ray diffraction. For DSC measurements, the samples were preheated to the molten state and then cooled at $20^{\circ}\text{C min}^{-1}$ to room temperature. The sample thus prepared are referred to as ‘scan-cooled’ samples. This procedure minimises any complication due to thermal history. The thermal transitions can then be related to the polymer structure directly. The results of DSC measurement obtained are shown in Fig. 3.

Homopolymer PB10: For this material three major peaks can be observed by DSC, at 197, 209 and 266°C . There is, in addition, a weak transition between those at 209 and 266°C . Optical microscopy studies of these systems were made difficult by the rather limited changes in texture. As a consequence we have used the classification of Asrar et al. [28] who have defined the following changes to be of note:

1. (i) $T_{(a)}$, the transition temperature at which the crystalline phase transformed to a deformable birefringent state;
2. (ii) $T_{(b)}$, the temperature at which both anisotropic and isotropic phase coexists;
3. (iii) $T_{(i)}$, the temperature at which the entire system became isotropic.

At room temperature, the PB10 polymer showed featureless birefringence. On heating, the behaviour corresponded closely to that observed from DSC measurements, and by

other workers. At the first transition temperature, 210°C , a deformable, birefringent, but very viscous state was observed. The polymer became highly fluid at 245°C . Above this temperature anisotropic and isotropic phases coexisted; the birefringence eventually disappeared at 270°C . Immediately after cooling down from the isotropic phase, needle-like crystals were observed at 253°C , these had a positive optical sign and correspond closely to the batonnets described by Asrar et al. [28].

Unfortunately, the textures observed could not be readily related to any liquid crystalline phase and consequently the material was studied further using X-ray scattering techniques. In particular it was intended to resolve the uncertainty as to the nature of the high temperature phases i.e. nematic [29,30], or smectic [20,28,31]. The X-ray scattering patterns obtained on heating the PB10 polymer are shown in Fig. 4. At low temperature two peaks could be observed, the appearance of the curves changed markedly on heating. The peak at low angle disappeared above 250°C , but below this temperature its position remained unaffected by heating. As this represents a tilted packing structure on the basis of the modelling studies described above, we can take the presence of this feature in the fluid polymer at high temperature to be indicative of a smectic phase. At higher angle, a sharp diffraction peak was observed. This gradually broadened with the increase of the temperatures until a broad diffuse peak was observed at 270°C .

Single-ring containing homopolymers CB10 and Q10: the phase behaviour for these homopolymers was much simpler than observed for PB10, in that only a single transition in DSC was observed in each case (Fig. 3a and b).

For the Q10 homopolymer DSC revealed a single transition, at 143°C , and optical microscopy showed that the sample became isotropic over the temperature range $145\text{--}155^{\circ}\text{C}$. No evidence for any liquid crystalline behaviour was obtained and polymer before melt appeared to be highly crystallised in agreement with X-ray diffraction shown.

The CB10 homopolymer shows a transition at 57°C by DSC in the first heating run. The material is soft and birefringent at room temperature. It was rather difficult to get a clear indication of the phase behaviour since the material was slow to crystallise. On heating in the microscope hot-stage, the polymer began to flow at 50°C and became completely isotropic at 60°C . In the scan-cooled sample of this material, only a relatively weak transition at ca. 40°C was observed using DSC. On the basis of these observations and the X-ray scattering data described above we can suggest that this material is ordered at room temperature (i.e. semicrystalline), but this order is severely disrupted by the presence of the side-groups and presumably there are kinetic factors which further hamper crystallization (see later).

Copolymers: The differences in phase behaviour between the PB10 homopolymer and the samples with low concentrations of the single ring system, i.e. PB9CB1 and PB9Q1,

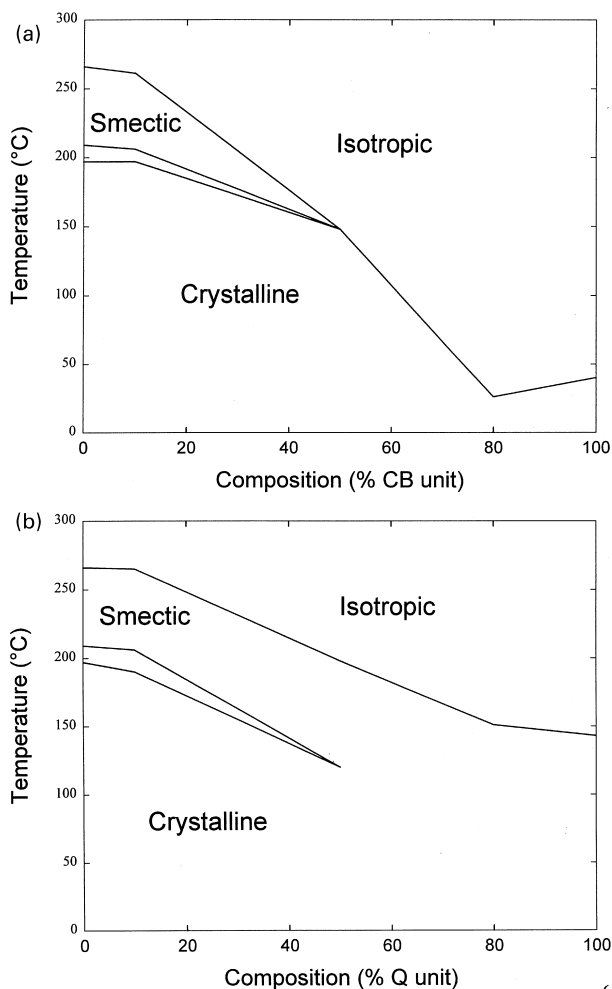


Fig. 5. Schematic phase diagrams of the PB-CB (a) and PB-Q (b) copolymer series.

were relatively small. Three peaks were observed by DSC, albeit with slightly reduced transition temperatures relative to the homopolymer. In the optical microscope these polymers behave in a similar fashion to the PB10 polymer and changes in texture were at best gradual. Thus, although it would seem likely that these materials also exhibit a mesophase, it is not possible to infer the mesophase type solely on the basis of these observations. However, by comparison with the homopolymer a smectic structure would seem most likely.

As the concentration of the side chain containing units increases for the CB series, rather complex solidification processes become apparent. There is no longer any sign of the liquid crystalline phase in 50% CB polymer, only a broad transition extending from just below the crystallisation melting point almost to room temperature. Further increase in the concentration of side-chain containing units, as in PB2CB8, resulted in a clear reduction in both transition temperature and its heat of fusion. It would appear however the phase behaviour was not very dissimilar to CB10, surprisingly the statistical implications [13,14] of

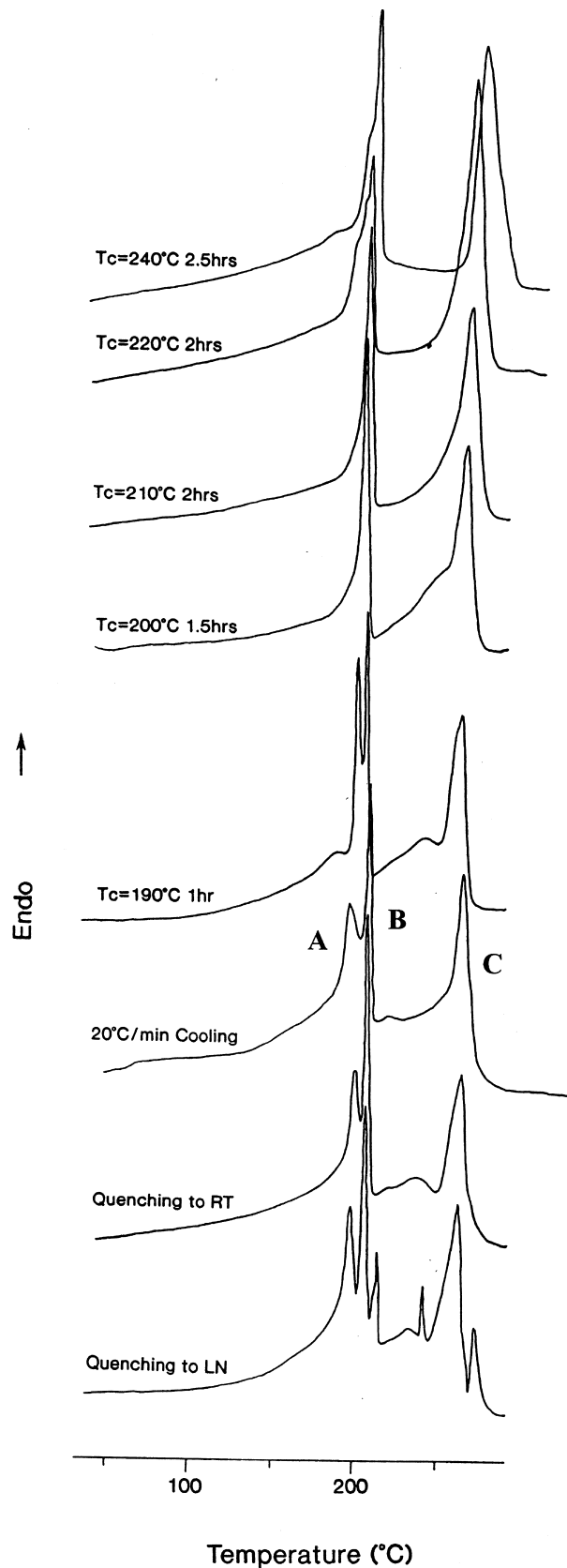


Fig. 6. DSC transitions of the PB10 polymer during heating scan after melting at 300°C and then quenched or isothermally crystallised at the conditions indicated.

copolymerisation does not appear to contribute markedly to the behaviour of these samples. The small enthalpy change for both PB2CB8 and CB10 suggest that the crystals provided only a minor component of the sample.

Copolymer with 50% hydroquinone-based comonomer also resulted in a complete disruption of the liquid crystal phase, as was found for the CB series. Here however, there is a much sharper crystalline to isotropic transition than that of PB5CB5, at a temperature only slightly below that observed for the biphenyl homopolymer, and a larger enthalpy change. This suggests that crystallinity is high in this copolymer. The materials containing higher concentrations of the single-ringed system also appeared to be highly crystalline, and though the melting transition occurred over a broader range than found for the homopolymer, the broadness was nothing like that found for the side-chain containing system.

In general the DSC investigations indicate that the homopolymers and the materials with small (10–20%) proportions of the copolymer show very similar phase behaviour. The 50/50 copolymers in contrast show rather different phase behaviour compared to the homopolymers, the broad DSC trace was a particular feature.

The investigation of the phase behaviour shows clearly that, with incorporation of the short hydroquinone units into the copolymer, the ordering was disturbed. Largely this reflected statistical considerations arising from copolymerisation. Side-chain bearing systems have a much more marked influence on the ordered phases. For the CB series increasing the number of side-chains onto the polymers increasingly disrupts crystallization. This serious disruption was observed even in the homopolymer CB10. Thus the phase behaviour reflects two major influences, namely, the packing difficulties arising from the side-chains, and the disorder introduced by copolymerisation. Of these two it would appear for this system, at least, the former has the more disruptive effect. Schematic phase diagrams are shown in Fig. 5.

4.4. Crystallisation of PB10

The discussion above gives broad outline of the phase behaviour of the two polymer series. However, transitions obtained from a single scan-cooled sample do not provide

an explanation for the double transition peaks around 200°C of PB10 polymers. For the scan-cooled sample, three peaks were observed by DSC, both on heating and cooling, indicative of independent processes arising from differently ordered structures. These transitions depend strongly on the thermal history. Systematic studies were made using specimens of different thermal history. These were prepared by first melting the polymers at 300–320°C and then quenching or annealing at a particular temperature. The transitions obtained by DSC are shown in Fig. 6. When the polymer was isothermally crystallised at temperatures lower than the transition labelled A, peak A is sharpened, while isothermal crystallisation at temperatures higher than A, resulted in the merging of transitions A with B. This suggests that the peaks A and B arise from rather similar structural transformation processes and that the structure giving rise to peak A can be suppressed under certain crystallisation conditions.

Further inspection was also made carefully using two specimens: one crystallised using scan-cooled conditions, the other isothermally at 210°C. These were studied using DSC at various scanning rates. The data are summarised in Table 4. A number of points were noted: firstly, there is no distinct effect of scanning rate on transition temperatures on either sample; secondly, the total enthalpies of the transition A and B from the scan-cooled samples remained constant at different scanning rates, but the enthalpy of the last transition increased gradually as the scanning rate gradually decreased; thirdly, the enthalpies of all transitions from the isothermally crystallised sample were independent of scanning rates. These results showed an overall increase in crystallinity from isothermally crystallised samples and the population of smectic structure (represented by transition C) was also dependent on the crystallinity.

Multiple thermal behaviour is a common phenomenon in many polymers. For example, in early studies of polystyrene three transition peaks were observed, these have been explained as melting of the secondary crystals, melting of the main population and the melting of the reorganised material [32,33]. Multiple-peak behaviour, however, is much more complicated in polymers with aromatic rings in the main chain, such as polyesters, like PET [34,35], PEN [36], poly(ether ketone)s such as PEEK [37,38],

Table 4
Scanning rate dependence of the thermal transitions from PB10 polymer (Note: The errors of the enthalpies were within $\pm 10\%$.)

Scan-cooled sample (cooling rate 20°C/min)						Isothermally crystallized sample ($T_c = 210^\circ\text{C}$)				
Scanning rate ($^\circ\text{C min}^{-1}$)	T_1 ($^\circ\text{C}$)	T_2 ($^\circ\text{C}$)	$\Delta H_1 + \Delta H_2$ (kcal mol^{-1})	T_3 ($^\circ\text{C}$)	ΔH_3 (kcal mol^{-1})	T_2 ($^\circ\text{C}$)	ΔH_2 (kcal mol^{-1})	T_3 ($^\circ\text{C}$)	ΔH_3 (kcal mol^{-1})	T_4 ($^\circ\text{C}$)
5	198	208	2.3	265	2.3	205	3.4	272	4.9	282
10	197	208	2.2	264	2.1	205	3.3	269	5.0	
20	198	208	2.3	263	1.4	205	3.0	268	4.5	
40	198	209	2.2	263	1.4	206	3.2	268	4.7	
80	198	210	2.3	264	1.6	207	3.2	270	5.0	

poly(ester amide)s [39–41] and also some rigid polymers with pendent side groups or side chains [42,43]. A number of explanations have been given for these multiple peaks. These include: one original crystal type undergoing processes of recrystallisation or reorganization [35]; two distinct original crystalline phases [36]; one crystalline phase in different morphologies arising from primary and secondary crystallization [37,38]; and transitions between mesophases [40–43].

In spite of the wide range of possible origins for multiple thermal behaviour described above, this seems to be an unusual phenomenon. X-ray scattering clearly shows that there are no different crystallisation phases present in the PB10. However, reorganisation and the secondary crystallisation also seem inadequate explanations for the behaviour, as both would be expected to show a scan-rate dependence in the DSC.

4.5. Isothermal crystallisation of PB5CB5 and morphology study

The thermal transition was found to be even more complicated in the copolymers, particularly the side-chain bearing copolymer PB5CB5. The most notable feature was found to be the unusually broad appearance of the thermal transition for the scan-cooled sample (see also Ref. [18]). For such a broad transition the origin at the high temperature end of the transition, may be different to that at the lower temperature end. In order to understand the nature of the crystallisation processes, the sample was isothermally crystallised at a range of temperatures and the influence on the subsequent thermal behaviour of the polymer was measured. It was found that for samples crystallised at a single temperature, a sharp peak appeared some 15–20°C above this temperature and was superimposed on the broad transition, with the higher and lower parts of the transition remaining. (see Fig. 2 in Ref. [18]) In order to explore this further, we prepared specimens by isothermally crystallising at multiple temperature steps. In these samples, the pattern is repeated several times, with reproducible and distinct multiple transitions as shown in Fig. 7. In the two step specimen (b) we see the sharp peak 1a formed at 160°C, melting at 177°C, with the broad remainder of the endotherm 1b. The subsequent treatment at 80°C has split the lower part of the endotherm into the relatively sharp peak 2a at 104°C and the broader 2b corresponding to the pair 1a and 1b at the higher temperatures. It is likely that the b peaks developed during the cooling process just as in scan-cooled samples, but the a peaks developed slowly, and resemble the peaks formed during secondary crystallisation [44] of PEEK [37] and other polymers. Peak 3 is the continuation of the normal endotherm down to room temperature. In the four step specimen (e) the peaks are more crowded and for peaks 3 and 4, the a and b components are not easily distinguished. The behaviour observed here is the characteristic of a material whose chemically varying components have a range of

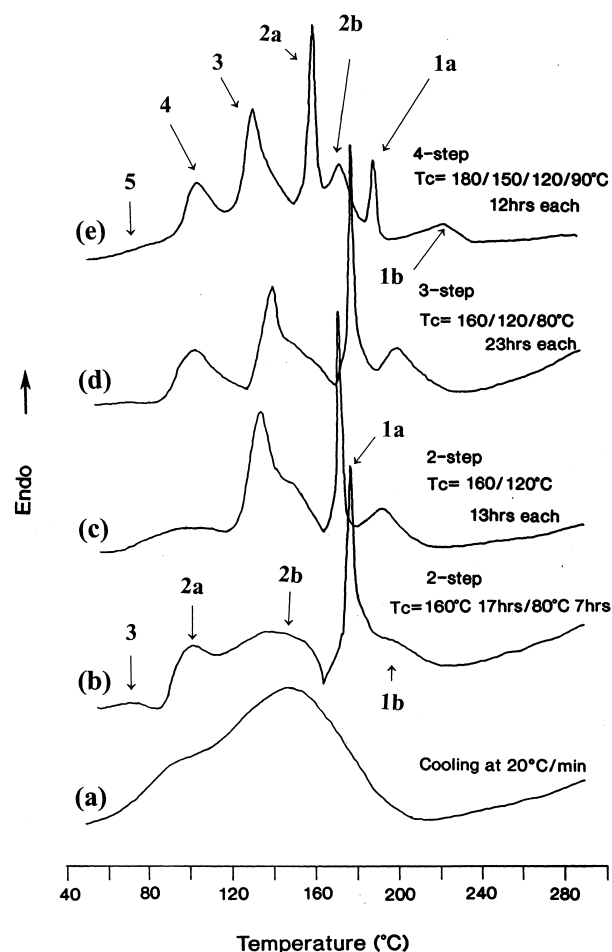


Fig. 7. DSC transitions of the PB5CB5 polymer after crystallisation at the conditions as follows: (a) scan-cooled; (b) and (c) two-step isothermal crystallisation at temperatures as indicated; (d) three-step isothermal crystallisation at temperatures as indicated and (e) four-step isothermal crystallisation at temperatures as indicated.

ability to order into material of any given thermal stability, with some lesser variation in terms of fast and slow ordering processes. The easily manipulation of peak temperatures with no fixed reference points is quite contrary to the situation where there are distinct crystalline forms each with its own characteristic melting point [45]. Sharp peaks at high annealing temperatures are also characteristic of branched polyethylene undergoing chemical segregation [46]. Although between treatments the peaks differ in shape and position, the total enthalpy was rather similar and found to be 70% of the value shown for the homopolymer PB10 after isothermal crystallisation. X-ray diffraction was also investigated but there were no distinct changes at different temperatures except a gradual loss of order on increasing temperature. This behaviour is clearly unusual and is dissimilar to the examples of multiple transitions cited above.

The fact that there is no apparent increase in the total enthalpy of the transitions for PB5CB5 indicates the phase behaviour does not originate from secondary crystallisation,

as such behaviour generally increases the amount of crystallisation through further crystallisation of amorphous material. However, these transitions were very unusual in comparison with a typical crystallisation, in being able to shift almost monotonically with annealing temperature; behaviour expected from secondary crystallization [37].

In order to obtain further information about the peculiar crystallisation behaviour of the PB5CB5 polymer specifically and these copolymers in general, the morphology of isothermally crystallised specimens was studied using SEM. Although at the resolution of SEM, it is not possible to observe detailed lamellar structure, it is still possible to compare the observed features with that known from other polymers. A series of specimens was prepared for this purpose: these were isothermally crystallised at 80, 100, 120 and 160°C for about 16 h, etched and examined under the SEM. Their morphology is shown in Fig. 8 (Plates 1–4).

In the specimen crystallised at $T_c = 80^\circ\text{C}$ (Plate 1), a rough texture containing some sheaf-like spherulites was identified with a texture resembling crystallised PEEK [22]. Not all objects appear sheaf-like, because the surface can intersect the sheaf at an angle or off centre. Therefore, it is reasonable to suggest that these have developed from well-spaced nuclei by the usual mechanism of spherulitic growth [46]. In the specimen crystallised at higher temperatures, $T_c = 160^\circ\text{C}$ (Plate 4), only a large quantity of parallel lamellar-like features were observed. The textures changed gradually with the isothermal crystallisation temperature.

From 80 to 120°C, sheaf-like structures are seen, increasing in size with the increase in crystallisation temperature. The level of organisation also appeared greater at higher crystallisation temperature (compare Plates 1 and 3). From the DSC data in Fig. 7; at high crystallisation temperatures, a much more limited fraction of the material has crystallised prior to quenching. Therefore, what is being crystallised is a more dilute system, which would be expected to give rise to parallel stacks of lamellae instead of branching spherulites, and most of the space is filled with material crystallised on quenching. These very open structures are more like those seen in polymer blends [47], a consequence of the system being dilute.

4.6. Structure formation processes from multiple thermal transitions

It is seen that the PB10 and the PB5CB5 polymers represent two extreme crystallisation behaviour in the PBCB family. To explain this, individual monomer sequence lengths have to be taken into account. For PB5CB5, the degree of polymerisation is low (Table 2) with the number-average value estimated to be about 5. If copolymerisation is random then the chance of a chain of 5 units consisting solely of PB would only be 1 in 32 (approximately 3%), and similarly for chains consisting only of 5 CB units. A statistical prediction based on

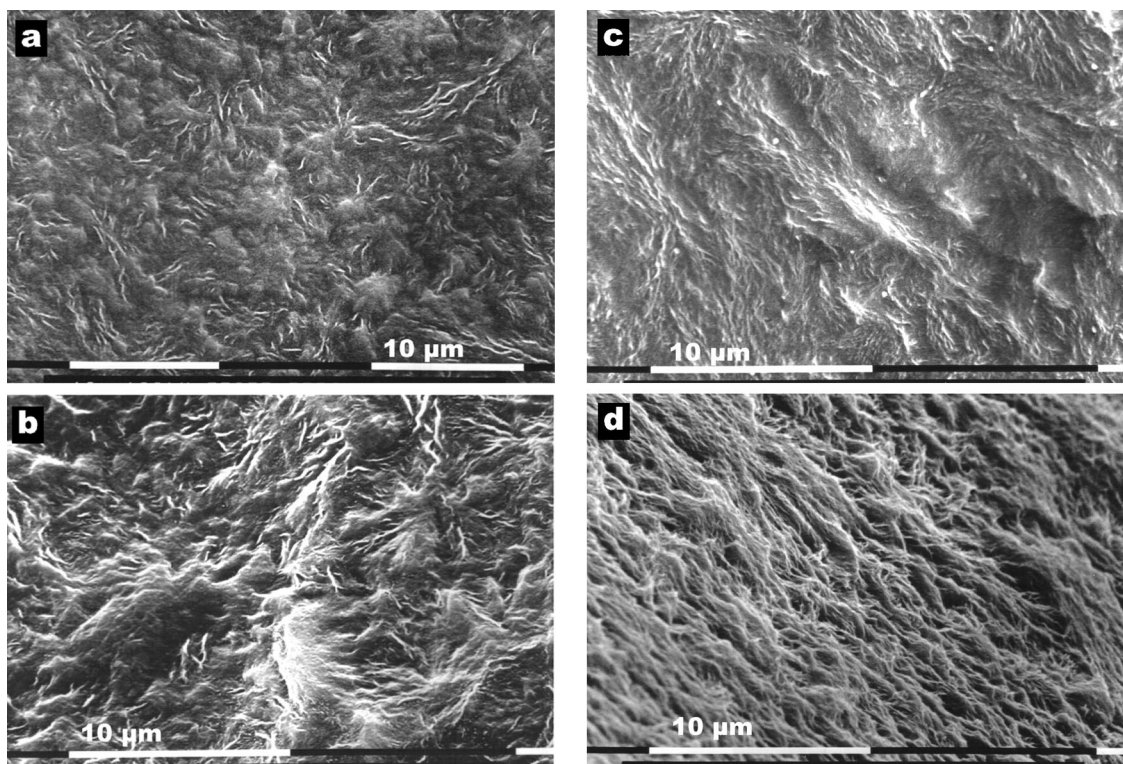


Fig. 8. Scanning electron microscopy of PB5CB5 sample after isothermal crystallisation at (Plate a) 80°C, (Plate b) 100°C, (Plate c) 120°C and (Plate d) 160°C.

unconditional probabilities [26] suggests that the average sequence length of PB5CB5 is limited to about 3, even if the degree of polymerisation is much higher. In consequence, only a very limited fraction of crystalline structures can form in this material. These sequences provide a broad range of molecular species with different interactions, which would contribute to the broad transitions of the scan-cooled sample and the multiple transition peaks of the isothermally crystallised samples. In the other word, this peculiar phase phenomenon may be the result of phase segregation, by matching of identical or similar sequence units.

It is now possible to explain what we found for the PB5CB5 copolymer. The range of the phase transition from the scan-cooled PB5CB5 sample extends from the melting point of the PB10 sample to the melting point of the CB10 sample. Thus the end points of the transition are due to the homopolymer structures. Thus it seems clear there are partially segregated clusters of homopolymer sequences. The origin of the broad transition observed from the scan-cooled sample, and also the multiple sharp-peaks observed from step isothermal crystallisation is thus clear. Different melting points arise from segregated clusters of different sequences of copolymers across the whole range of distributions. Because of this structural complication, crystallisation is very slow. Isothermal crystallisation provides the conditions required to reorganise these structures. The crystal formed by the segregation or match of identical or near-identical chemical structure units in copolymer sequences has been termed as non-periodic crystalline layer structure [18].

The process of structural formation is a thermodynamic as well as kinetic process. A particular condition normally favours one kind of structure formation. The number of the structures formed depends on firstly the chemical structure of the polymer itself. These chemical structures determine the interaction force between the chains, and therefore the speed of structure formation. Hence the structure formed under a certain condition can also be affected or even governed by kinetic factor. In terms of the rate of structural formation, PB10 polymer is a typical model of fast structural formation, and PB5CB5 polymer typical of a slow one. They form a good example to show the competition between the thermodynamic and the kinetic processes.

The phases found in PB10 are presumably thermodynamically as well as kinetically favoured. The interaction between the polymer chains are strong and so the annealing at scan-cooled condition are not fast enough to freeze many structure information. The side chains in the PB5CB5 copolymer certainly disturb the polymer chain–chain interaction and slow down the crystallisation process. Phases, or order, can be formed based on many structural segments at a range of crystallisation conditions, such as annealing temperatures.

5. Conclusions

Two series of aromatic copolyesters were prepared. In one series, PB-Q, the proportions of a biphenyl and a phenyl unit was varied through copolymerisation; in the second series, PB-CB, the phenyl ring system was further substituted with an aliphatic side-chain. These were used to study property change resulting from pendant side-chain groups and from disorder into the polymer backbone by copolymerisation.

The semi-quantitative solubility measurement gives a clear picture of relative influence of the two disrupting systems. The introduction of side-chains is a much more effective method of improving solubility than disruption through copolymerisation. The crystallinity may partially responsible for it. The level of the crystallisation in solid state materials of both copolymer series was monitored using X-ray diffraction. Upon increasing temperature, the phases of the polymers, though complicated due to chemical structure factors, show interesting phenomenon which became the focus point of our study. The PB10 and the PB5CB5 samples show distinct different multiple transitions. It is concluded through experimental investigation that they are two extreme examples in the family to show the fast and the slow crystallisation. The crystallisation is now understood to be the segregation of individual sequences of the polymer; the non-periodic lattice model, i.e. non-heterogeneous crystallites are formed through lateral matching of similar units.

Despite the low degree of polymerisation of the copolymers examined, the result do reveal a practical approach which may be taken to modify the properties of rigid polymers through molecular engineering.

Acknowledgements

This work formed part of the Courtaulds Polymer Science Prize Programme at the University of Reading.

References

- [1] Tanner D, Gabard V, Schaefer JR. In: *Polymers for Advanced Technologies*; IUPAC International Symposium, 1988:384.
- [2] Morgan PW. *Macromolecules* 1977;10:1381.
- [3] Kwolek SL, Morgan PW, Schaefer JR, Gulrich LW. *Macromolecules* 1977;10:1390.
- [4] Du Pont (Kwolek SL). British Patent, 1,283,064.
- [5] Jaffe M, Jones SR. In: Lewin M, Preston J, editors. *High technology fibres, Part A*. New York: Dekker, 1985.
- [6] Ballauff M. *Angew Chem, Int Ed Engl* 1989;28:253.
- [7] Lewis DN, Fellers JF. In: Zachariades AE, Porter RS, editors. *High modulus polymers*. New York: Marcel Dekker, 1988.
- [8] Kricheldorf HR, Schwartz G. *Polym Bull* 1979;1:383.
- [9] Marvel CS, Hartzell GE. *J Am Chem Soc* 1969;81:448.
- [10] Kovacic P, Lange RM. *J Org Chem* 1963;28:968.

- [11] Antoun S, Lenz RW, Jin J-I. *J Polym Sci, Polym Chem Ed* 1981;19:1901.
- [12] Jackson Jr. WJ, Kuhfuss HF. *J Polym Sci, Polym Chem Ed* 1976;14:2043.
- [13] Flory PJ. *J Chem Phys* 1947;15:684.
- [14] Flory PJ. *J Chem Phys* 1949;17:223.
- [15] Windle AH, Viney C, Golombok R, Donald AM, Mitchell GR. *Faraday Discuss Chem Soc* 1985;79:55.
- [16] Hanna S, Windle AH. *Polymer* 1988;29:2076.
- [17] Zhou Q-F, Lenz RW. *J Polym Sci, Polym Chem Ed* 1983;21:3313.
- [18] He Z, Mitchell GR. *Polymer* 1994;35:1322.
- [19] He Z, Davis FJ, Mitchell GR. *Eur Polym J* 1996;32(6):735.
- [20] Blumstein A, Sivaramkrishnam KN, Blumstein RB, Clough SB. *Polymer* 1982;23:47.
- [21] Mitchell GR, Davis FJ, Ashman AS. *Polymer* 1987;28:639.
- [22] Bassett DC, Olley RH, Blundell DJ. *Polymer* 1986;27:344.
- [23] Tsai Ruey-shi, Tsai Hong-bing. *J Macromol Sci, Phys B* 1992;31(4):485.
- [24] Jones TPH, Mitchell GR, Windle AH. *Colloid Polym Sci* 1983;261:110.
- [25] Narten AH. *J Chem Phys* 1977;67:2102.
- [26] Mitchell GR, Windle AH. *Colloid Polym Sci* 1985;263:230.
- [27] Golombok R, Hanna S, Windle AH. *Mol Cryst Liq Cryst* 1988;155:281.
- [28] Asrar J, Toriumi H, Watanabe J, Krigbaum WR, Ciferri A, Preston J. *J Polym Sci, Polym Phys Ed* 1983;21:1119.
- [29] Van Luyen D, Strzelecki L. *Eur Polym J* 1980;16:303.
- [30] Blumstein A, Sivaramkrishnam KN, Clough SB, Blumstein RB. *Mol Cryst Liq Cryst* 1979;49:255.
- [31] Krigbaum WR, Watanabe J, Ishikawa T. *Macromolecules* 1983;16:1271.
- [32] Overbergh N, Berghmans H, Smets G. *J Polym Sci (C)* 1972;38:237.
- [33] Overbergh N, Berghmans H, Reynaers H. *J Polym Sci, Polym Phys Ed* 1976;14:1177.
- [34] Wunderlich B. *Macromolecular physics, Crystal melting*, vol. 3. New York: Academic Press, 1980.
- [35] Holdsworth PJ, Turner-Jones A. *Polymer* 1970;12:195.
- [36] Buchner S, Wiswe D, Zachmann HG. *Polymer* 1989;30:480.
- [37] Bassett DC, Olley RH, Al Raheil IAM. *Polymer* 1988;29:1745.
- [38] Cheng SZD, Wu ZQ, Wunderlich B. *Macromolecules* 1987;20:2802.
- [39] He Z, Whitcombe MJ, Mitchell GR. *Br Polym J* 1990;23:41.
- [40] Aharoni SM. *Macromolecules* 1988;21:1941.
- [41] Aharoni SM. *Macromolecules* 1989;22:686.
- [42] Majnusz J, Lenz RW. *Eur Polym J* 1989;25:847.
- [43] Majnusz J, Lenz RW. *Eur Polym J* 1992;28:253.
- [44] Yagpharov M. *J Therm Anal* 1986;31:1073.
- [45] He Z, Olley RH. *Polymer* 2000;41:1157.
- [46] Bassett DC. *Principles of Polymer Morphology*. Cambridge, 1981.
- [47] Barham PJ, Hill MJ, Keller A, Rosney CCA. *J Mater Sci Lett* 1988;7:1271.